American Mineralogist, Volume 81, pages 385–394, 1996

# Protons in the magnesium phosphates phosphoellenbergerite and holtedahlite: An IR and NMR study

FABRICE BRUNET* AND TORSTEN SCHALLER

Bayerisches Geoinstitut, Universität Bayreuth, D-95440 Bayreuth, Germany

## ABSTRACT

Two structurally related magnesium phosphates, phosphoellenbergerite ($P6_3mc$) and holtedahlite ($P6_3$), have been investigated using a combination of high-frequency IR and $^1$H MAS, $^{31}$P MAS, and $^{31}$P CP MAS NMR spectroscopy on synthetic material. For phosphoellenbergerite, the two proton sites, H1 and H2, detected in single-crystal XRD studies, are confirmed. The protons on the first site, H1, delocalized around the threefold axis, form OH groups with the unshared apical O atom of $PO_4$ tetrahedra. Those on the second site, H2, belong to $Mg_2O_8OH$ dimers of face-sharing Mg octahedra, which form double chains. The spectroscopic data reveal additional protons (H3) in phosphoellenbergerite. By combining both crystallographic and spectroscopic data, it can be inferred that the H3 protons are associated with Mg vacancies in the single chains of face-sharing Mg octahedra. Furthermore, a quantitative inspection of signal intensities indicates that the proton sites in synthetic phosphoellenbergerite are not all saturated. Therefore, the substitution $P^{5+} = Si^{4+} + H^+$ might account for part of the Si-P replacement in the silicate-to-phosphate ellenbergerite series. The results obtained for the proton distribution in holtedahlite, $Mg_2PO_4OH$, were used as a reference to facilitate the interpretation of the IR and NMR spectra of phosphoellenbergerite.

## INTRODUCTION

The ellenbergerite series is a complete silicate-to-phosphate solid-solution series, which occurs in a coesite-bearing terrane of the Western Alps (Dora-Maira). The silicate end-member, $[Mg_{1/3},(Ti,Zr)_{1/3},\square_{1/3}]_2Mg_6Al_6Si_2Si_6O_{28}(OH)_{10}$, is stable only above 27 kbar (Chopin 1986; Chopin et al. 1992), whereas the phosphate end-member, $(Mg_{0.9},\square_{0.1})_2Mg_{12}P_2P_6O_{38}H_{8.4}$, is stable down to 10 kbar (Brunet et al. 1996). The P/Si ratio in natural ellenbergerite is therefore a valuable indicator of minimum pressure of metamorphism (Chopin and Sobolev 1995). However, all the coupled substitutions that are possible to replace Si by P in the ellenbergerite structure have not been determined. The role of protons and vacancies especially needs to be clarified. The coupled substitution $^{[6]}Al^{3+} + {}^{[4]}Si^{4+} = {}^{[6]}Mg^{2+} + {}^{[4]}P^{5+}$ most efficiently replaces Si with P (Chopin et al. 1986). However, because the silicate end-member contains only six Al, this substitution mechanism cannot account for the replacement of more than six Si. Tetravalent cations (Ti, Zr) and protons, as well as octahedral vacancies, must also contribute to charge balance beyond that of Si-P replacement. From single-crystal X-ray diffraction (XRD) studies along the series (Klaska 1985; Chopin et al. 1986; Comodi and Zanazzi 1993; Amisano-Canesi 1994), two proton sites have been identified, but they cannot account for all the protons in the structure. Additional protons are probably bonded to the single chains of face-sharing octahedra that are partially vacant (Comodi and Zanazzi 1993). It is expected that these protons form OH groups with the O atoms of the vacant octahedra, as is the case for staurolite (Hawthorne et al. 1993) and magnesiodumortierite (Ferraris et al. 1995; Chopin et al. 1995), as well as for hydrogarnets with O atoms of vacant Si tetrahedra (Lager et al. 1989). To complement the XRD studies of the ellenbergerite structure, we investigated the synthetic phosphate end-member of the ellenbergerite series (phosphoellenbergerite, IMA vote 94–006) using infrared (IR) and nuclear magnetic resonance (NMR) spectroscopic methods. We chose the phosphoellenbergerite end-member rather than any other composition along the series mainly because of its chemical simplicity: (1) The phosphoellenbergerite composition belongs to a three-component system, $MgO$-$P_2O_5$-$H_2O$, whereas Si-bearing ellenbergerite compositions require at least two additional components, namely $Al_2O_3$ and $SiO_2$. (2) Each cation site in phosphoellenbergerite is occupied by only one atomic species: P, Mg, or H. Furthermore, single-crystal diffraction data have already been collected on synthetic phosphoellenbergerite (Amisano-Canesi 1994).

NMR spectroscopy and IR spectroscopy have been successfully used to locate protons in minerals (e.g., Kalinichenko et al. 1987; Yesinowski et al. 1988; Cho and Rossman 1993). Although $^{31}$P NMR has been widely ap-

* Present address: Laboratoire de Géologie, 5, rue Kessler, F-63038 Clermont-Ferrand, France.

0003–004X/96/0304–0385$05.00

plied in investigations on protonated phosphates (Bleam et al. 1989; Lagier et al. 1992; Hartmann et al. 1994), $^{25}$Mg MAS NMR is seldom used (Dupree and Smith 1988; MacKenzie and Meinhold 1994), and so only a few reference data are available. Herein, we applied a combination of various one-dimensional solid-state NMR techniques. First, we used $^{1}$H high-speed magic-angle-spinning (MAS) NMR to observe directly the protons in the structure. Second, information about the protons was obtained indirectly by using $^{31}$P CP MAS NMR to investigate cross-polarization (CP) dynamics. Third, because the protonation of $PO_4$ tetrahedra significantly influences the parameters of the chemical-shift tensor, we inspected the $^{31}$P MAS NMR spectrum at low spinning frequencies, which provided further constraints for the short-range geometry.

Interpretation of the IR and NMR data was facilitated using synthetic holtedahlite, $Mg_2PO_4OH$, as an analog because holtedahlite and phosphoellenbergerite are structurally related (Rømming and Raade 1989). Most of the measurements reported here were performed on both compounds.

## Experimental methods

### Synthesis of phosphoellenbergerite and holtedahlite

Phosphoellenbergerite and holtedahlite were synthesized in a piston-cylinder apparatus using conventional talc-pyrex assemblies. The products were identified by X-ray powder diffraction. The starting material was enclosed with 10–20 wt% deionized water in a large-volume silver capsule sealed with friction-fitting lids. Synthesis of single-phase phosphoellenbergerite was achieved at 800 °C and 30 kbar (46 h). The starting material was an oxide mixture of $NH_4H_2PO_4$ + MgO in an 8 to 13.75 molar ratio, heated beforehand at 600 °C for 3 h in a platinum crucible.

A second batch of synthetic phosphoellenbergerite was obtained at 900 °C, 30 kbar (44.5 h) with excess $D_2O$. Starting material and $D_2O$ were enclosed in an arc-welded gold capsule, and the experiment was conducted in a dried NaCl-based pressure cell.

The starting material for the synthesis of holtedahlite was an equimolar mixture of $Mg_3(PO_4)_2 \cdot 8H_2O$, dehydrated at 950 °C, and MgO. To overcome metastable growth previously encountered in the $Mg_2PO_4OH$ polymorphic system (Raade 1990), seeds of holtedahlite were added to the starting mixture. Despite this precaution, the first experiment of 88 h at 17 kbar and 750 °C yielded three phases: holtedahlite, althausite (a polymorph of $Mg_2PO_4OH$), and an unidentified phase occurring in trace amounts. This product, after grinding, was held under the same *P-T* conditions for 72 additional hours, causing althausite to disappear. The unidentified trace phase remained. The presence of this phase might reflect a slight stoichiometry offset, but because of its small amount, another synthesis with new starting material was not considered necessary.

### IR spectroscopy

The IR spectra of single crystals were measured with a Bruker 120 high-resolution FTIR spectrometer with a tungsten source and a $CaF_2$ beam splitter. The IR beam was focused using the optics of a Bruker IR microscope. The sample was placed on a glass slide, for which the background effect was corrected by subtraction. Polarized IR measurements were performed on two oriented phosphoellenbergerite single crystals using a beam slit to reduce the angle of convergence to ~10°. The phosphoellenbergerite and holtedahlite synthetic crystals investigated here are about 80 μm long and 30 μm thick. All the spectra were recorded using between 100 and 5000 scans.

### NMR spectroscopy

All NMR experiments were performed with a Bruker MSL 300 spectrometer with a 4 mm double-bearing CP MAS probe ($^{1}$H MAS spectra at 300.1 MHz, $^{31}$P MAS and CP MAS spectra at 121.5 MHz). Because the sample amount (30–50 mg) was insufficient to fill the rotor, the spectra were collected using a Kel-F insert designed to fit exactly inside the rotor (Merwin et al. 1989). The $^{1}$H MAS spectra were measured using single-pulse excitation with a 90° pulse delay of 5 μs and a recycle delay of 10 s (120 and 360 transients for holtedahlite and phosphoellenbergerite, respectively). To separate spinning sidebands from the isotropic signals, a spinning frequency of 9–10 kHz was necessary. The $^{1}$H chemical shifts are reported relative to an external tetramethylsilane (TMS) standard equal to 0 ppm; the $^{31}$P chemical shifts are referred to an aqueous solution of monophosphoric acid (85%). The $^{31}$P single-pulse MAS spectra were recorded using 3.5 μs pulses (90°), a relaxation delay of 90 s, and spinning frequencies of 1.6–10.0 kHz. The spectra obtained at lower spinning frequencies were used to determine the parameters of the chemical-shift tensor. These parameters were calculated using a computer program that fits the spinning-sideband intensities according to Maricq and Waugh (1979). All $^{31}$P CP MAS experiments with variable contact times used a spinning frequency of 3.6 kHz, a $^{1}$H 90° pulse of 3.0 μs, and a recycle delay of 10 s. The contact times ranged from 50 μs to 300 ms; each spectrum was obtained with 240 transients. Peak intensities were determined using a computer program that fits the spectra to a sum of Lorentzian and Gaussian curves with optimized peak position, peak shape, and peak width.

## Outline of the phosphoellenbergerite and holtedahlite structures

### Phosphoellenbergerite structure

The phosphoellenbergerite structure was refined by Amisano-Canesi (1994) using a synthetic single crystal produced at 1000 °C and 30 kbar. The structure (space group, $P6_3mc$) consists of two main structural units: double chains (or ribbons) formed by pairs of face-sharing Mg octahedra (M2) linked by edges, and single chains of

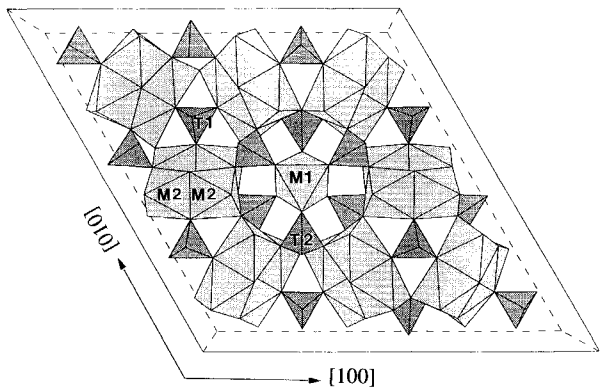


FIGURE 1. View along the *c* axis of the phosphoellenbergerite structure displaying the single-chain face-sharing Mg octahedra (M1) surrounded by $PO_4$ tetrahedra (T2).

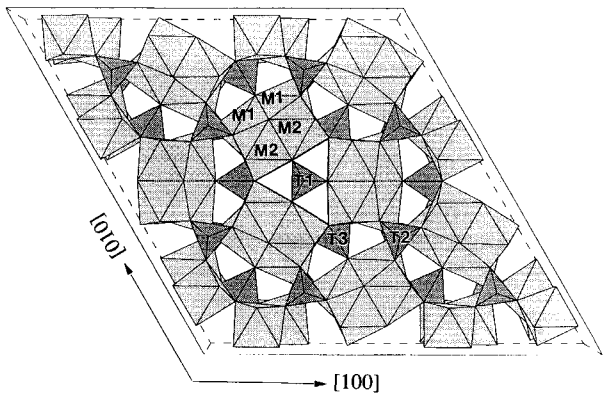


FIGURE 2. View along the *c* axis of the holtedahlite structure.

face-sharing Mg octahedra (M1). Both extend along the *c* direction. These octahedral chains are linked by corner sharing to the P tetrahedra (Fig. 1).

P atoms are distributed over two tetrahedral sites; T1 is on the threefold axis and forms an OH phosphate group with a proton, denoted H1. This tetrahedron shares three O atoms (O6) with the three surrounding double chains, and its fourth O atom (O7) forms the OH group, OH1. The T2 tetrahedra connect the single chains to the double chains. It should be noted that each corner (O4) of an octahedron of the single chains is shared with a T2 tetrahedron.

Bond-valence calculations indicate a charge deficiency of about one valence unit for two O atoms (O7 and O5), which are, therefore, presumably protonated (Amisano-Canesi 1994). The H1 proton attached to O7 is delocalized around the threefold axis and was not detected on the difference-Fourier map, in contrast to the H2 proton attached to the O5, which was clearly observed (Amisano-Canesi 1994). The O5 atom belongs to the double chains and is common to four M2 octahedra. Assuming the two proton sites, H1 and H2, are fully occupied, they account for eight protons per formula unit (pfu) (H1 × 2 and H2 × 6). Therefore, approximately 0.4 additional protons (5% of the total proton content) are required to balance the charge associated with the ~10% Mg vacancies in the M1 octahedral site (Amisano-Canesi 1994; Brunet et al. 1996). Hence, a third proton site (H3) must be considered. The small amount of extra protons makes it difficult to propose proton-acceptor O atoms on the basis of bond-strength calculations only. The situation is different for the silicate end-member, in which about two additional protons (i.e., five times more than in phosphoellenbergerite) are present when the two sites, H1 and H2, are saturated. Bond-strength calculations suggest that these extra protons are bonded to the O4 of the single chains (Comodi and Zanazzi 1993). It is likely that the O4H groups are attached to vacant octahedra in the single chains (cf. staurolite in which the M3 octahedral site is occupied by either an Al or by two protons: Hawthorne et al. 1993). In phosphoellenbergerite, if protons are bonded to the O4 of vacant octahedra, then some of the T2 tetrahedra are protonated.

### Holtedahlite structure

The holtedahlite structure was refined using both synthetic and natural crystals by Rømming and Raade (1989). Holtedahlite ($Mg_2PO_4OH$, space group $P6_3$), like phosphoellenbergerite, exhibits protonated ribbons of dimers of face-sharing $MgO_6$ octahedra associated with OH phosphate groups (Fig. 2). In phosphoellenbergerite, all the M1-M1 dimers are identical, whereas in holtedahlite two nonequivalent dimers are present, M1-M1 and M2-M2, which alternate by edge sharing along the *c* direction. The single proton site, H2, attached to the double chains in phosphoellenbergerite is split into two sites, H2a and H2b, in the holtedahlite structure [in the original work of Rømming and Raade (1989), the sites are referred to as H1 and H2]. The H2b site faces the channel formed by three ribbons, as does H2 in phosphoellenbergerite. The OH group OH2a on the other side of the double chain faces a different atomic environment. However, the first O neighbors for the H2a and H2b sites belong to the double chain, and, therefore, the first O coordination shells of these sites are closely related. Significant differences in the O environment of H2a and H2b occur only at O-H ··· O distances longer than 3.2 Å, for which hydrogen bonding is very weak (Table 1).

The channel defined by the three ribbons encloses an $HPO_4$ group (T1 site) in a way similar to that in phosphoellenbergerite, and the corresponding proton site is also referred to as H1. There are two other P sites, T2 and T3, which link the groups of three ribbons to each other. Single chains of face-sharing octahedra do not exist in holtedahlite. Therefore, the single-chain proton site of phosphoellenbergerite, provisionally noted H3, has no equivalent in holtedahlite. There are seven possible proton positions in the holtedahlite structure (H2a × 3, H2b × 3, and H1 × 1), although the structure contains only six protons pfu. Therefore, not all proton sites are fully occupied. On the basis of bond-strength calculations,

**TABLE 1.** Comparison of the O-H···O distances in holtedahlite and phosphoellenbergerite

| Holtedahlite | | Phosphoellenbergerite | |
|---|---|---|---|
| OH2a-OH2b | 2.66* | OH2-OH2 | 2.71* |
| OH2a-O5 | 2.67* | OH2-O6 | 2.73* |
| OH2a-O2 × 2 | 2.84* | OH2-O3 | 2.85* |
| OH2a-O4 × 2 | 2.86* | OH2-O3 | 2.93* |
| OH2a-O6 × 2 | 3.56* | OH2-O2 | 3.15* |
| OH2a-O5 | 3.42 | no equivalent | |
| OH2a-O6 | 3.56 | no equivalent | |
| OH2b-OH2a | 2.73* | OH2-OH2 | 2.71* |
| OH2b-O1 | 2.76* | OH2-O6 | 2.73* |
| OH2b-O2 × 2 | 2.82* | OH2-O3 | 2.85* |
| OH2b-O4 × 2 | 2.90* | OH2-O3 | 2.93* |
| OH2b-O3 × 2 | 3.11* | OH2-O2 | 3.15* |
| OH2b-OH1 | 3.23 | OH2-OH1 | 3.17 |
| OH2b-O1 | 3.28 | OH2-O6 | 3.26 |
| OH1-O1 × 3 | 2.50* | OH1-O6 | 2.50* |
| OH1-OH2b | 3.23 | OH1-OH2 | 3.17 |
| OH1-O3 | 3.25 | OH1-O2 | 3.39 |
| OH1-O1 | 3.27 | OH1-O6 | 3.29 |

* Edge of the coordination polyhedra to which the OH group belongs. The OH2b in holtedahlite faces the $HPO_4$ group.

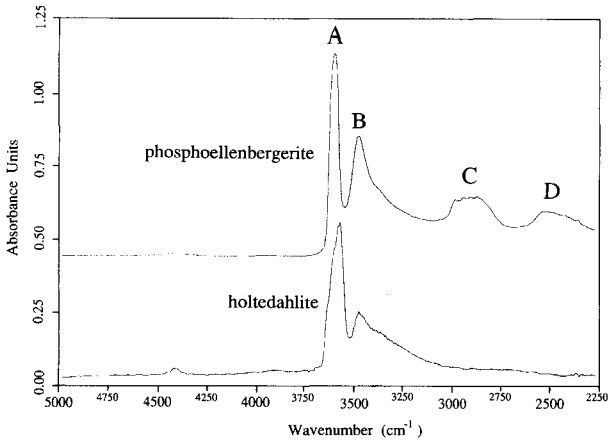


**FIGURE 3.** Single-crystal IR spectra of phosphoellenbergerite and holtedahlite (100 and 500 scans, respectively). Note that band A is truncated for both phases.

Rømming and Raade (1989) proposed an occupancy of ~85% for each proton site, leading to the structural formula $Mg_{12}[HPO_{4(x)},PO_{4(1-x)}](PO_4)_2(PO_4)_3(O_x,OH_{6-x})$, with $x = 0.85$.

## RESULTS AND DISCUSSION

### The infrared spectra of phosphoellenbergerite and holtedahlite

The infrared spectrum of a natural holtedahlite was measured by Raade and Mladeck (1979), and the OH-stretching modes were later analyzed on the basis of the structure determination (Rømming and Raade 1989). In the OH-stretching region, the spectrum of synthetic holtedahlite (Fig. 3) is very similar to that of natural holtedahlite. It consists of a strong band (A) at 3567 $cm^{-1}$, which displays fine structure, and an asymmetric band (B) at 3472 $cm^{-1}$. The lower frequency absorption band was not observed by Rømming and Raade (1989), although it has significant intensity. If this band is considered, the previous assignment must be modified. It is expected that the stretching modes of OH2a and OH2b lie in the same wavenumber region because both protons are in a similar atomic environment attached to the double chains (Table 1). We assume that the fine structure of band A results from the contribution of these two protons, and, consequently, band B can be assigned to the H1 proton of the OH phosphate group.

The two main bands of the holtedahlite spectrum have analogous bands at 3593 and 3476 $cm^{-1}$ in the spectrum of phosphoellenbergerite, but two additional bands occur at lower frequencies, near 2910 $cm^{-1}$ (C) and 2500 $cm^{-1}$ (D). The absorption band B assigned to the H1 protons is almost identical to its homolog in the holtedahlite spectrum, with the same stretching frequency and peak shape. Band A differs slightly in the two spectra; the peak maxima are shifted, and the peak shape is particularly different. The fine structure of band A in the holtedahlite spectrum is absent in the phosphoellenbergerite spectrum, which is characterized by a sharper band A. These features are consistent with the proton-distribution model deduced from the X-ray diffraction data. The atomic environment of the H1 site is identical in the two structures, and so the corresponding OH-stretching bands are also identical. The H2 site in phosphoellenbergerite resembles sites H2a and H2b in holtedahlite, thus similar stretching frequencies are expected. Although the fine structure of band A results from the contribution of two twin proton sites in holtedahlite, the contribution of a single well-defined proton site produces a sharper band in the phosphoellenbergerite spectrum. Because bands A and B in the phosphoellenbergerite spectrum are attributed to H2 and H1, respectively, the low-frequency bands, C and D, should be assigned to additional protons. In the IR spectrum of partially deuterated phosphoellenbergerite (Fig. 4), additional bands C′ and D′ occur at lower wavenumbers (2145 and 1850 $cm^{-1}$, respectively), as expected for OD stretching modes ($\nu_{OH}/\nu_{OD} = 1.36$ for C and $\nu_{OH}/\nu_{OD} = 1.35$ for D). Polarized infrared measurements of two oriented crystals of phosphoellenbergerite (~30 $\mu$m thick), one cut along $c$ and the other cut perpendicular to $c$, show that the vibration vector associated with bands C and D, has a component along the $c$ direction and in the $a$-$b$ plane (001).

The frequency range containing bands A and B (3600–3475 $cm^{-1}$) in both minerals suggests that the corresponding protons are only engaged in very weak hydrogen bonds. This interpretation agrees with the crystal-structure data that indicate that neither of the OH groups, OH1 and OH2, in phosphoellenbergerite has an O atom closer than 3.2 Å suitable for hydrogen bonding (Table

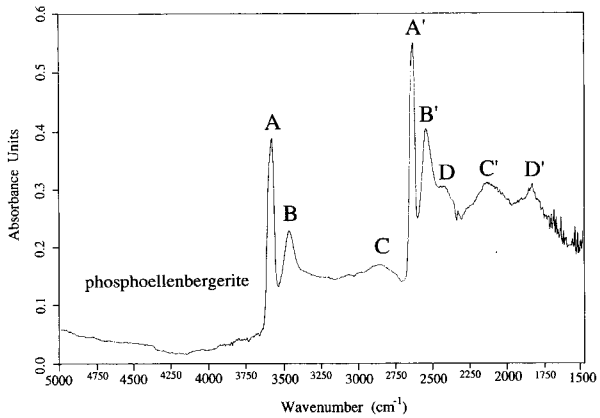


FIGURE 4. Single-crystal IR spectrum of partially deuterated phosphoellenbergerite (5000 scans).

1). From the frequencies of bands C and D, one can derive OH3 ··· O distances of 2.7 and 2.6 Å, respectively, using the empirical correlation curve of Nakamoto et al. (1955). These distances, however, are incompatible with those obtained from the diffraction study, in which the distances between O atoms that can accept a proton are all longer than 2.9 Å. Therefore, these protons are associated with defects that are probably octahedral vacancies where the structure is locally distorted.

### $^1$H MAS NMR experiments

In the $^1$H MAS NMR spectra of phosphoellenbergerite and holtedahlite (Fig. 5), we can distinguish three resonances: an intense signal at about 1.2 ppm (A), a much smaller signal at 4.5 ppm (B), and a peak at 11 ppm (C). Although the first two signals appear in both spectra, the resonance at 11 ppm occurs only in the spectrum of phosphoellenbergerite. The resonance at 4.5 ppm is not well resolved in phosphoellenbergerite, but it is easily identified by its spinning-sideband pattern, which differs considerably from the pattern of the 1.2 ppm resonance.

Given the structural considerations discussed above and the results obtained by IR spectroscopy, we propose the following assignment for these three resonances (Table 2): The isotropic chemical shift and the intensity of the signal at 1.2 ppm in both spectra indicate that this resonance results from H2 protons bonded to the double chains. The resolution of the $^1$H MAS spectrum of holtedahlite allows estimation of the relative peak intensities. Fitting the centerband and all spinning sidebands up to the second order, we obtained a relative intensity of 83 ± 5%, which is in good agreement with the proton distribution proposed by Rømming and Raade (1989). Furthermore, this assignment is supported by NMR investigations on brucite, $Mg(OH)_2$ (Sears et al. 1988), and on the synthetic end-member pargasite (Welch et al. 1994), which report isotropic chemical shifts of 0.5 and 1.2 ppm, respectively.

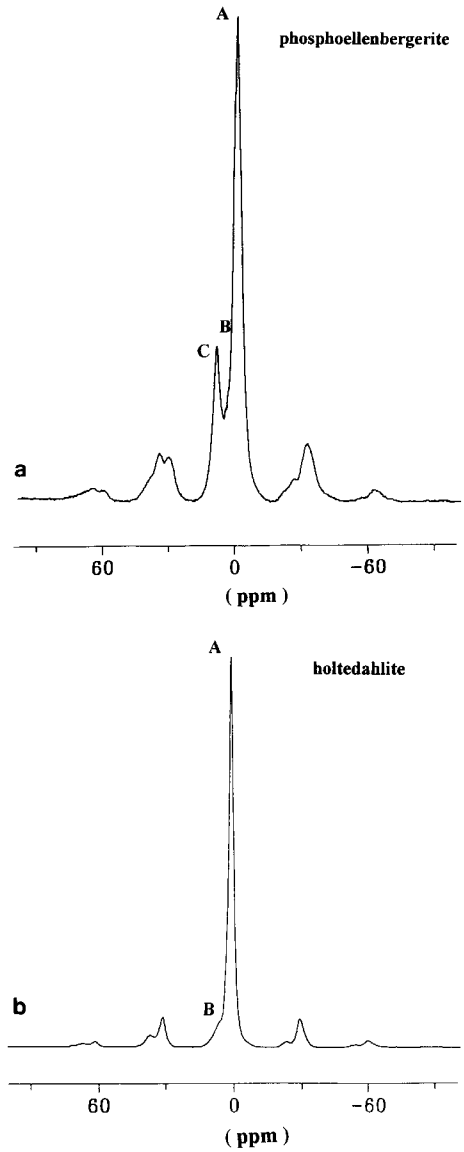


FIGURE 5. The $^1$H MAS NMR spectra of (a) phosphoellenbergerite and (b) holtedahlite recorded at a spinning frequency of 10.0 kHz. Note that only resonances A and B show spinning sidebands.

TABLE 2. Results of IR and $^1$H NMR spectroscopy

| IR | | $^1$H NMR | | | |
|---|---|---|---|---|---|
| Resonance | Wavenumber ($cm^{-1}$) | Resonance | $\delta_{iso}$ (ppm) | $I/I_{total}$* | Assignment |
| | | **Holtedahlite** | | | |
| B | 3472 | B | 4.5 | 0.17 | H1 |
| A | 3567 | A | 1.2 | 0.83 | H2a + H2b |
| | | **Phosphoellenbergerite** | | | |
| B | 3476 | B | 4.5 | 0.88 | H1 |
| A | 3593 | A | 1.2 | | H2 |
| C, D | 2910, 2500 | C | 11.0 | 0.12 | H3 |

* Estimated error for the intensities is ±0.05.

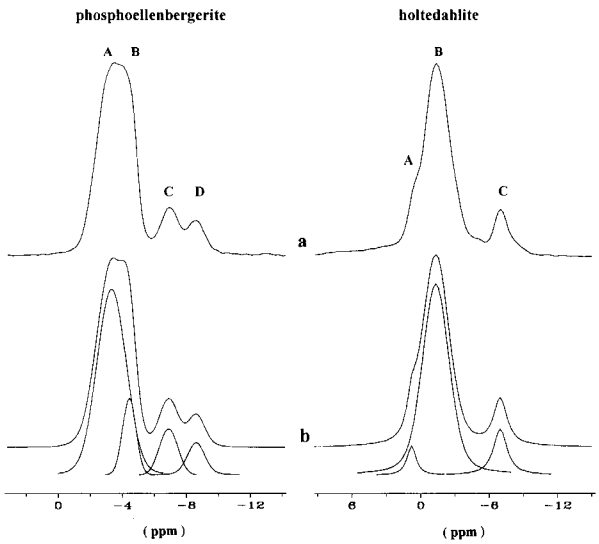


FIGURE 6. The $^{31}P$ MAS NMR spectra of phosphoellenbergerite and holtedahlite. (a) Spectra recorded at a spinning frequency of 10 kHz, (b) deconvolution of a using sum of four and three Lorentzian and Gaussian lines, respectively.

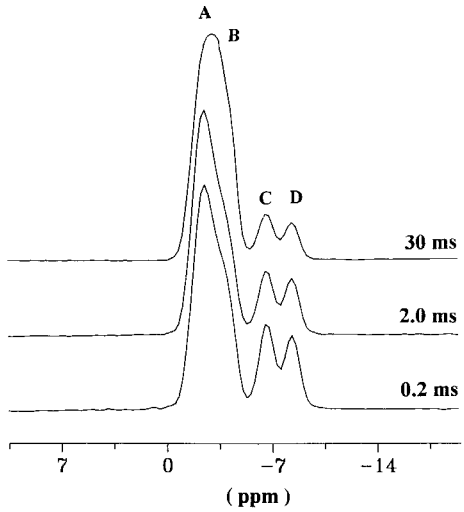


FIGURE 7. The $^{31}P$ CP MAS NMR spectra of phosphoellenbergerite at contact times of 0.2, 2.0, and 30 ms.

Consequently, the resonance at 4.5 ppm must be assigned, in both spectra, to the apical proton of the T1 tetrahedron. Although this H1 signal appears as a distinct shoulder in the spectrum of holtedahlite, it is overlapped by the resonance at 11 ppm in the phosphoellenbergerite spectrum.

The main difference between the $^{1}H$ MAS spectra of holtedahlite and phosphoellenbergerite is the signal at 11 ppm in the latter. Therefore, this resonance results from the additional H3 protons. The isotropic chemical-shift value indicates that this resonance is due to protons engaged in hydrogen bonding. Given the results of empirical studies (Eckert et al. 1989) and theoretical calculations (Berglund and Vaughan 1980; Sternberg and Brunner 1994), the chemical shift observed here corresponds to an O-H3 ··· O distance of about 2.65 Å. This result is corroborated by the IR measurements. It should be noted that the resonance at 11 ppm has no spinning sidebands, which indicates a higher mobility for H3 than for the other protons of the structure.

To constrain the H3 site population, the signal at 11 ppm was fitted with a sum of Lorentzian and Gaussian curves yielding a value of 12 ± 5% (Table 2). However, there are two main problems inherent to the fitting procedure. First, due to their larger line widths and the poorer signal-to-noise ratio of the spinning sidebands, the intensity of the resonances at 1.2 and 4.5 ppm is prone to underestimation. Second, it is known that relative intensities depend strongly on the choice of a line-shape function (Mahler and Sebald 1995). Given the spectral resolution obtained here, we cannot determine this function with certainty. Therefore, the choice of Lorentzian and Gaussian line shapes is somewhat arbitrary.

## $^{31}P$ MAS experiments and $^{31}P$ CP MAS NMR experiments

Using high sample-spinning frequencies in $^{31}P$ NMR experiments on phosphates, one usually observes only the isotropic resonances and can estimate the relative signal intensities; however, information is lost about the chemical-shift anisotropy, which monitors subtle changes in the environment of the nucleus. Spinning the sample at moderate frequencies and fitting the spinning-sideband intensities according to the procedure of Maricq and Waugh (1979) allows us to determine the chemical-shift tensor components, which are expected to be different for the P sites in the ellenbergerite structure.

Furthermore, the P sites are expected to be affected by different H-P dipolar interactions. These differences can be monitored by cross-polarization experiments made at various contact times; the build-up of $^{31}P$ magnetization with cross-polarization rate $T_{CP}^{-1}$ is a direct measure of the strength of the dipolar $^{1}H$-$^{31}P$ interaction, which is, to a first approximation, a function of the internuclear distance. The dependence of the $^{31}P$ magnetization on the contact time $\tau_m$ can be described as

$$M(\tau_m) = \frac{M_0}{1-\lambda}\cdot\left[\exp\left(\frac{-\tau_m}{T_{1\rho}(^{1}H)}\right) - \exp\left(\frac{-\tau_m}{T_{CP}}\right)\right] \quad (1)$$

where $\lambda = T_{CP}/T_{1\rho}(^{1}H)$ and $M_0$ represents the maximum $^{31}P$ magnetization in the absence of $^{1}H$ spin-lattice relaxation in the so-called rotating frame, characterized by the relaxation time $T_{1\rho}(^{1}H)$. The relaxation time $T_{1\rho}(^{31}P)$ is assumed to be long in comparison with $T_{CP}$ and $T_{1\rho}(^{1}H)$.

The $^{31}P$ MAS spectra of holtedahlite and phosphoellenbergerite recorded at a spinning frequency of 10.0 kHz are depicted in Figure 6. Both spectra show three apparent resonances. In the holtedahlite spectrum, we observe a low-field shoulder at 0.7 ppm, an intense signal at −1.8 ppm, and a resonance at −7.0 ppm. In the spectrum of

**TABLE 3.** Results of $^{31}P$ CP MAS and $^{31}P$ MAS experiments

| Resonance | $\delta_{iso}$ (ppm) | $T_{CP}$ (ms) | $T_{1\rho}$ (ms) | $I/I_{total}$* | Abundances from XRD data** | Assignment |
|---|---|---|---|---|---|---|
| | | | **Phosphoellenbergerite** | | | |
| B | −4.4 | 0.98 ± 0.08 | 99 ± 10 | 0.13 | T1:0.25 | $P1O_4$ |
| C | −7.0 | 0.12 ± 0.02 | 104 ± 10 | 0.11 | | $P1O_4H1$ |
| A | −3.3 | 0.41 ± 0.03 | 93 ± 8 | 0.68 | T2:0.75 | $P2O_4$ |
| D | −8.7 | 0.15 ± 0.02 | 101 ± 9 | 0.08 | | $P2O_4H3$ |
| | | | **Holtedahlite** | | | |
| A | 0.7 | | | 0.06 | T1:0.17 | $P1O_4$ |
| C | −7.0 | | | 0.11 | | $P1O_4H1$ |
| B | −1.8 | | | 0.83 | T2 + T3:0.83 | $P2O_4 + P3O_4$ |

* Estimated error for the intensities is ±0.03.
** Data for phosphoellenbergerite from Amisano-Canesi (1994), for holtedahlite from Rømming and Raade (1989).

phosphoellenbergerite, a broad and intense resonance at about −3.8 ppm is observed; two smaller, well-resolved signals at −7.0 and −8.7 ppm are also present.

Phosphoellenbergerite and holtedahlite contain both protonated and unprotonated $PO_4$ tetrahedra. The protonation of phosphates generally leads to a shift of the isotropic signal toward lower frequencies, i.e., more negative $\delta_{iso}$ values (Bleam et al. 1989). We are, therefore, tempted to separate the resonances of the two spectra into two groups with respect to their chemical shifts: One group comprises the resonances in the range of 1 to −4 ppm, assigned to the unprotonated $PO_4$ molecules, and the other group includes resonances between −7.0 and −8.7 ppm, which represent the protonated $PO_4$ tetrahedra. Obviously, both spectra show a similar resonance at −7.0 ppm, suggesting an identical P site in the two structures. This result reflects the similarity of the T1 site in the phosphoellenbergerite and holtedahlite structures.

Figure 7 shows the $^{31}P$ CP MAS spectra of phosphoellenbergerite measured at various contact times. Surprisingly, we not only find different dependencies for both groups of signals on the contact time, but we also observe a significant change in the line shape of the signal at −3.8 ppm: At short contact times, a shoulder appears at −4.4 ppm, which increases relative to the other signals at longer contact times. This indicates that the signal centered around −3.8 ppm consists of two resonances with slightly different isotropic chemical shifts but significantly different cross-polarization characteristics. Fitting these spectra, we obtained two resonances at −3.3 and −4.4 ppm. To determine the cross-polarization rate, $T_{CP}^{-1}$, and the relaxation time, $T_{1\rho}$, the relative signal intensities were determined for 40 spectra. The results obtained by fitting these spectra are listed in Table 3. The resonances at −7.0 and −8.7 ppm have, within the experimental error, the same cross-polarization time, which is very similar to time constants for protonated phosphates such as crandallite, $CaAl_3(PO_4)_2(OH)_5 \cdot H_2O$, and wavellite, $Al_3(PO_4)_2(OH)_3 \cdot 5H_2O$, that have cross polarization times of 0.16 and 0.17 ms, respectively (Bleam et al. 1989). The time constants for the resonances at −3.3 and −4.4 ppm are considerably larger, reflecting a smaller H-P dipolar coupling.

The results obtained by the cross-polarization experiment confirm our assumption that the resonances at −7.0 and −8.7 ppm are due to protonated $PO_4$ tetrahedra, whereas the two high-field resonances represent nonprotonated phosphate groups. This assumption was also confirmed by a slow-spinning $^{31}P$ MAS experiment using $^1H$ high-power decoupling. Figure 8 depicts the spectrum of phosphoellenbergerite recorded at a spinning frequency of 1670 Hz. The spinning-sideband pattern of the low-field resonances differs considerably from the pattern observed for the high-field signals. Because the resonances at −7.0 and −8.7 ppm and their sidebands are sufficiently resolved, we fitted all observable sideband intensities and determined the chemical-shift tensor parameters using a computer program that fits these intensities according to the procedure of Maricq and Waugh (1979). For comparison, the chemical-shift parameters were also determined for the resonance at −7.0 ppm in the $^{31}P$ MAS spectrum of holtedahlite. The results, listed in Table 4, show that the site of the observed $^{31}P$ nucleus is significantly distorted. We obtained an anisotropy of the chemical-shift tensor of −69 to −83 ppm and an asymmetry parameter $\eta$ of about 0.3, which reflects distortion from axial symmetry due to the protonation of these tetrahedra. The values obtained for phosphoellenbergerite and holtedahlite (Table 4) show that the local symmetry around the observed nuclei is similar for both compounds, thus corroborating our signal assignment. Furthermore, asymmetry and anisotropy values approach those obtained for $HPO_4$ groups (Hartmann et al. 1994).

The information obtained by CP experiments, in particular the isotropic chemical shift and the line width of the four signals in the $^{31}P$ NMR spectrum of phosphoellenbergerite, can be used to determine the relative signal intensities in the $^{31}P$ MAS NMR spectrum recorded at 10.0 kHz. Although the resonances assigned to nonprotonated $PO_4$ tetrahedra have a relative intensity of approximately 81%, 19% of the total intensity ($I_{total}$) is due to protonated tetrahedra (Table 3).

In contrast to the phosphoellenbergerite spectra, the relative intensities in the $^{31}P$ MAS NMR spectrum of holtedahlite (Fig. 6b) can be determined independent of the cross-polarization experiments. Here, the relative in-

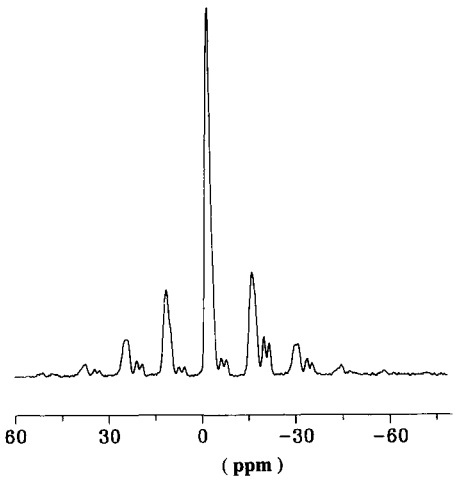


FIGURE 8. The $^{31}P$ MAS NMR spectrum of phosphoellenbergerite obtained at a spinning frequency of 1.67 kHz.

tensities are approximately 6% for the shoulder at 0.7 ppm, 83% for the most intense signal (−1.8 ppm), and 11% for the resonance at −7.0 ppm. To test the consistency of the NMR and X-ray diffraction data, we compared these intensities to those expected from the P and proton distribution proposed by Rømming and Raade (1989) for holtedahlite. The assignment of the three $^{31}P$ resonances to the three P sites (T1, T2, and T3) leads to a discrepancy with respect to signal intensity because ⅙ of the total P content is incorporated into the T1 site, ⅓ into the T2 site, and ½ into the T3 site. However, the sum of the intensity contributions of the P atoms belonging to the T2 and T3 sites equals the intensity of the resonance at −1.8 ppm, indicating that these atoms account for this resonance (Table 3). Consequently, two resonances (0.7 and −7.0 ppm) must be attributed to a single crystallographic site (i.e., T1). The partial occupancy of the H1 sites can be inferred to explain this feature. When the proton site is occupied, T1 is an $HPO_4$ group. The corresponding $^{31}P$ resonance is expected to occur at low frequencies (see above) and would therefore produce the −7.0 ppm signal. The resonance at 0.7 ppm is attributed to the H-free T1 site ($PO_4$ group). According to the intensities that we derived for the latter resonances, the occupancy of H1 is approximately 65% (i.e., $x = 0.65$ in the formula of holtedahlite). Similar reasoning can be applied to assign the $^{31}P$ MAS NMR spectrum of phosphoellenbergerite (Table 3). Four resonances were identified: The resonances at −3.3 and −4.4 ppm are attributed to P atoms of unprotonated tetrahedra, and the resonances at −7.0 and −8.7 ppm are assigned to P atoms of $HPO_4$ groups. The resonance at −7.0 ppm in both phosphoellenbergerite and holtedahlite spectra is assigned to P atoms of the T1 site in both structures. In the phosphoellenbergerite structure, because H2 is bonded to $MgO_6$ octahedra, only H3 is able to form additional $HPO_4$ groups (T2 site) that can account for the signal at −8.7 ppm. With respect to the high-frequency bands, the assignment can be twofold. First, the occurrence of two bands (−3.3 and −4.4 ppm) can be explained by the existence of two chemical environments for the P atoms of the unprotonated T2 sites (i.e., the protonation of the T2 site by the H3 protons would correspond to a third environment). A second option is to assume a partial occupancy of the H1 proton site leading to unprotonated T1 sites, as previously shown for holtedahlite, which would account for the −4.4 ppm resonance. This option was adopted for the assignment presented in Table 3. In any case, the intensity of ~11% of the −7.0 ppm resonance is lower than the value of 25% expected if the H1 site is fully occupied. The uncertainty of the relative intensity derived from fitting these peaks is not greater than a few percent and alone cannot account for this difference. A partial occupancy of the H1 site implies that more protons should enter the H3 sites than was previously thought. This observation seems to be confirmed by the relatively high intensity (12 ± 5%) of the signal assigned to the H3 protons in the $^{1}H$ MAS NMR phosphoellenbergerite spectrum.

## CONCLUSION

Some of the proton sites (referred to as H3 in the present study) within the phosphoellenbergerite structure represent a very small proportion of the total proton content (0.4 H pfu) and are therefore difficult to detect using X-ray diffraction techniques. Using spectroscopic methods, we obtained distinctive signals, either directly from these protons (i.e., IR and $^{1}H$ NMR) or indirectly through the P signal (i.e., $^{31}P$ NMR) and the H-P interaction (i.e., $^{31}P$ CP MAS NMR). On the basis of a combination of X-ray diffraction and spectroscopic results, we propose the following proton distribution within the phosphoellenbergerite structure. The H3 protons are concentrated in the vicinity of structural defects likely to be the Mg octahe-

TABLE 4. The $^{31}P$ chemical-shift parameters of the protonated $PO_4$ tetrahedra

| | $\delta_{iso}$ (ppm) | $\sigma_{11}$ (ppm) | $\sigma_{22}$ (ppm) | $\sigma_{33}$ (ppm) | $\Delta\sigma$ (ppm) | $\eta$ |
|---|---|---|---|---|---|---|
| Phosphoellenbergerite | −8.7 | 24 | 14 | −64 | −83 | 0.18 |
| | −7.0 | 23 | 8 | −53 | −69 | 0.33 |
| Holtedahlite | −7.0 | 25 | 10 | −57 | −74 | 0.30 |

*Note:* Shielding tensor components are reported according to Haeberlen (1976): $\delta_{iso} = -\sigma_{iso}$; $|\sigma_{33} - \sigma_{iso}| \geq |\sigma_{11} - \sigma_{iso}| \geq |\sigma_{22} - \sigma_{iso}|$; $\eta = (\sigma_{22} - \sigma_{11})(\sigma_{33} - \sigma_{iso})^{-1}$; $\Delta\sigma = \sigma_{33} - \frac{1}{2}(\sigma_{11} + \sigma_{22})$. Estimated error for the chemical-shift tensor components is ±1 ppm, for $\eta$ ±0.01.

dral vacancies, where they form $HPO_4$ groups with the T2 tetrahedra. These protons are strongly hydrogen bonded (O-H ··· O = 2.6–2.7 Å). The corresponding O-H ··· O angles are expected to approach 180° (Pedersen 1974), and so these protons would vibrate along the unshared edges of the vacant octahedron.

The presence of two IR bands assigned to the H3 protons is not compelling evidence for the splitting of the H3 site into two sites. The occurrence of three bands in the low-frequency region (<3000 $cm^{-1}$) resulting from the contribution of a single proton site, has already been reported in hydrogen phosphates (Bratoz and Hadzi 1957).

The population of the H3 site cannot be precisely determined from our spectroscopic data. Charge balance requires an average of two protons per Mg vacancy if the H1 and H2 sites are fully occupied. The $^{31}P$ MAS measurement seems to indicate that, as in holtedahlite, the H1 site is partially vacant. For charge-balance reasons, the missing protons on that site must be located somewhere else in the structure and should therefore belong to the H3 sites. If so, there are on average more than two protons per octahedral vacancy in the phosphoellenbergerite structure. This is consistent with the tolerance of the octahedral site of the single chains with respect to the charge of the incorporated cations. In P-free ellenbergerite, up to ⅓ of this site can be populated by tetravalent cations such as Ti and Zr (Chopin et al. 1986). The partial occupancy of the H1 site in phosphoellenbergerite, as well as the ability of the H3 site to incorporate more than two protons per octahedral vacancy, may allow additional protons to enter the phosphoellenbergerite structure. Furthermore, a substitution such as $P^{5+} = Si^{4+} + H^+$ must also be considered among the substitution mechanisms that can concur with the P-Si replacement along the ellenbergerite series.

## Acknowledgments

F.B. was financially supported by an E.C. grant (Human Capital and Mobility Programme, ERB 4001GT933454) and the PROCOPE German-French Exchange Programme. We thank C. Chopin, F. Seifert, and H. Keppler for helpful discussions. Constructive reviews by C.A. Geiger, P. Schmid-Beurmann, J.R. Kirkpatrick, and an anonymous referee significantly improved the manuscript.

## References cited

Amisano-Canesi, A. (1994) Studio cristallografico di minerali di altissima pressione del complesso Brossasco-Isasca (Dora-Maira meridionale), 185 p. Ph.D. thesis, Università di Torino, Turin, Italy.

Berglund, B., and Vaughan, R.W. (1980) Correlations between proton chemical shift tensors, deuterium quadrupole couplings, and bond distances for hydrogen bonds in solids. Journal of Chemical Physics, 73, 2037–2043.

Bleam, W.F., Pfeffer, P.E., and Frye, J.S. (1989) $^{31}P$ solid-state nuclear magnetic resonance spectroscopy of aluminum phosphate minerals. Physics and Chemistry of Minerals, 16, 455–464.

Bratoz, S., and Hadzi, D. (1957) Infrared spectra of molecules with hydrogen bonds. Journal of Chemical Physics, 27, 991–997.

Brunet, F., Chopin, C., and Seifert, F. (1996) Phase relations in the MgO-$P_2O_5$-$H_2O$ system and stability of phosphoellenbergerite. Contributions to Mineralogy and Petrology, in press.

Cho, H., and Rossman, G.R. (1993) Single-crystal studies of low-concentration hydrous species in minerals: Grossular garnet. American Mineralogist, 78, 1149–1164.

Chopin, C. (1986) Phase relationships of ellenbergerite, a new high-pressure Mg-Al-Ti-silicate in pyrope-coesite quartzite from western Alps. Geological Society of America Memoir, 164, 31–42.

Chopin, C., Klaska, R., Medenbach, O., and Dron, D. (1986) Ellenbergerite, a new high-pressure Mg-Al-(Ti,Zr)-silicate with a novel structure based on face-sharing octahedra. Contributions to Mineralogy and Petrology, 92, 316–321.

Chopin, C., Schreyer, W., and Baller, T. (1992) Ellenbergerite stability: A reappraisal. Terra Nova (Abstract Supplement), 4, 10.

Chopin, C., Ferraris, G., Ivaldi, G., Schertl, H.-P., Schreyer, W., Compagnoni, R., Davidson, C., and Davis, A.M. (1995) Magnesiodumortierite, a new mineral from very-high-pressure rocks (western Alps): II. Crystal chemistry and petrological significance. European Journal of Mineralogy, 7, 525–535.

Chopin, C., and Sobolev, N. (1995) Principal mineralogical indicators of UHP in crustal rocks. In R.G. Coleman and X. Wang, Eds., Ultra high-pressure metamorphism, p. 97–131. Cambridge University Press, U.K.

Comodi, P., and Zanazzi, P.F. (1993) Structural study of ellenbergerite: Part I. Effects of high temperature. European Journal of Mineralogy, 5, 819–829.

Dupree, R., and Smith, M.E. (1988) Solid state magnesium-25 NMR spectroscopy. Journal of the Chemical Society, Chemical Communications, 1483–1485.

Eckert, H., Yesinowski, J.P., and Stolper, E.M. (1989) Quantitative NMR studies of water in silicate glasses. Solid State Ionics, 32/33, 298–313.

Ferraris, G., Ivaldi, G., and Chopin, C. (1995) Magnesiodumortierite, a new mineral from very-high-pressure rocks (Western Alps): Part I. Crystal structure. European Journal of Mineralogy, 7, 167–174.

Haeberlen, U. (1976) High-resolution NMR of solids: Selective averaging. In Advances in Magnetic Resonance, Supplement 1, p. 17–26. Academic, San Diego, California.

Hartmann, P., Vogel, J., and Schnabel, B. (1994) The influence of short-range geometry on the $^{31}P$ chemical shift tensor in protonated phosphates. Journal of Magnetic Resonance, A111, 110–114.

Hawthorne, F.C., Ungaretti, L., Oberti, R., Caucia, F., and Callegari, A. (1993) The crystal structure of staurolite: I. Crystal structure and site populations. Canadian Mineralogist, 31, 551–582.

Kalinichenko, A.M., Proshko, V.Ya., Matiash, I.V., Pavlishin, V.I., and Garmanik, M.Ya. (1987) NMR data on crystallochemical features of hydrogrossular. Geochemistry International, 24, 132–135 (translated from Geokhimiya, 9, 1363–1366, 1986).

Klaska, R. (1985) Strukturtopologien einiger Oxid-Kristalle, 181 p. Habilitationschrift, Ruhr-Universität Bochum, Germany.

Lager, G.A., Armbruster, T., Rotella, F.J., and Rossman, G.R. (1989) OH substitution in garnets: X-ray and neutron diffraction, infrared, and geometric-modeling studies. American Mineralogist, 74, 840–851.

Lagier, C.M., Olivieri, A.C., Apperley, D.C., and Harris, R.K. (1992) Magic-angle-spinning $^{31}P$ MAS NMR spectra of solid dihydrogen phosphates. Solid State Nuclear Magnetic Resonance, 1, 205–210.

Mahler, J., and Sebald, A. (1995) Deconvolution of $^{29}Si$ MAS NMR spectra of silicate glasses revisited: Some critical comments. Solid State Nuclear Magnetic Resonance, 5, 63–78.

MacKenzie, K.J.D., and Meinhold, R.H. (1994) $^{25}Mg$ nuclear magnetic resonance spectroscopy of minerals and related inorganics: A survey study. American Mineralogist, 75, 250–260.

Maricq, M.M., and Waugh, J.S. (1979) NMR in rotating solids. Journal of Chemical Physics, 70, 3300–3316.

Merwin, L.H., Sebald, A., Espidel, J.E., and Harris, R.K. (1989) An air-tight, inexpensive, easy-to-use MAS rotor insert. Journal of Magnetic Resonance, 84, 367–371.

Nakamoto, K., Margoshes, M., and Rundle, R.E. (1955) Stretching frequencies as a function of distances in hydrogen bonds. Journal of the American Chemical Society, 77, 6480–6488.

Pedersen, B. (1974) The geometry of hydrogen bonds from donor water molecules. Acta Crystallographica, B30, 289–291.

Raade, G. (1990) Hydrothermal syntheses of $Mg_2PO_4OH$ polymorphs. Neues Jahrbuch für Mineralogie Monatshefte, 289–300.

Raade, G., and Mladeck, M.H. (1979) Holtedahlite, a new magnesium phosphate from Modum, Norway. Lithos, 12, 283–287.

Rømming, C., and Raade, G. (1989) The crystal structure of natural and synthetic holtedahlite. Mineralogy and Petrology, 40, 91–100.

Sears, R.E.J., Kaliaperumal, R., and Manogaran, S. (1988) $^1$H shielding anisotropy in $Mg(OH)_2$: The isolated OH-group. Journal of Chemical Physics, 88, 2284–2288.

Sternberg, U., and Brunner, E. (1994) The influence of short-range geometry on the chemical shift of protons in hydrogen bonds. Journal of Magnetic Resonance, A108, 142–150.

Welch, M.D., Kolodziejski, W., and Klinowski, J. (1994) A multinuclear NMR study of synthetic pargasite. American Mineralogist, 79, 261–268.

Yesinowski, J.P., Eckert, H., and Rossman, G.R. (1988) Characterization of hydrous species in minerals by high-speed $^1$H MAS-NMR. Journal of the American Chemical Society, 110, 1367–1375.

Manuscript received May 10, 1995
Manuscript accepted October 31, 1995